X-643-68-264
PREPRINT

NASA TM X- 63307

ORBIT INFORMATION DERIVED FROM ITS HODOGRAPH

J. B. EADES, JR.

JULY 1968

GSFC — GODDARD SPACE FLIGHT CENTER —
GREENBELT, MARYLAND

X-643-68-264

ORBIT INFORMATION DERIVED FROM ITS HODOGRAPH

J. B. Eades, Jr.

July 1968

Goddard Space Flight Center

Greenbelt, Maryland

CONTENTS

Orbit Information Derived from Its Hodograph

J. B. Eades, Jr.*

NASA, Goddard Space Flight Center

Greenbelt, Maryland

ABSTRACT

The hodograph representing a two-body motion can be utilized to develop analytic relations descriptive of this category of central field trajectories. In this paper a brief vector development is presented which leads directly to the hodograph; also several interesting results are obtained which connect the various angles of reference and the speed components for the flight path. A correlation between the hodographs, referenced to a moving axis system (r, φ, z) and an orbital fixed axis system (x, y, z), is presented. Also, a geometric description of and correlation between the position angle of reference (true anomaly), the eccentric anomaly and the mean anomaly is developed.

*NRC-NASA Resident Research Associate, on leave from Virginia Polytechnic Institute, Blacksburg, Virginia; also Associate Fellow of AIAA.

NOTATION

$\mathcal{A}$, $\mathcal{P}$	describe apocenter and pericenter locations, resp.
a	semimajor axis length
B, B′	describe the extent of the semi-minor axis
$\mathcal{C}$, R	parameters associated with the hodograph (See equation (8))
$\mathbf{e}_i$	unit vector ($i = r, \varphi, z; x, y, z$).
E	specific energy for a body in motion ($E = V^2/2 - \mu/r$).
$\mathcal{E}$	eccentric anomaly
F, F^*	occupied, unoccupied foci.
h	specific angular momentum
M	mean anomaly
n	mean motion
P	a general position, referred to a trajectory
p	focal parameter ($p = h^2/\mu = a\lvert 1 - \epsilon^2 \rvert$)
Q, J, D, O	position indicators for constructions used herein
r	radius to a trajectory position, measured from F.
r, φ, z	polar coordinates, associated with the moving triad $\mathbf{e}_r$, $\mathbf{e}_\varphi$, $\mathbf{e}_z$
t	time
V, V_i	Velocity vector, speed components ($i = r, \varphi, x, y$)
$V(\varphi)$, V(y)	speed components defined with Fig. 2
x, y, z	cartesian coordinates, associated with the trajectory-fixed triad $\mathbf{e}_x$, $\mathbf{e}_y$, $\mathbf{e}_z$
β, γ	elevation angles referred to the V_x, V_y and V_r, V_φ speed components, resp.

ϵ, $\boldsymbol{\epsilon}$ eccentricity (scalar, vector)

μ gravitational constant

τ time of pericenter passage.

Subscripts, Superscripts

$( )_{lim}$ a limit value

$(\dot{})$, $(\ddot{})$ orders of differentiation, with respect to time.

INTRODUCTION

In recent years there has been a renewed interest in hodograph methods, especially as they refer to orbital mechanics and space flight. The works of Altman[1]*, Pistiner[2], Sun[3], and Eades[4] to mention a few have done much to advance the knowledge of this method, and to provide useful analytic and geometric tools for applications purposes.

It is generally thought that the hodograph is a novel technique used as a check on analytic methods; however, it has been employed as a means for providing relations between the various parameters used to describe orbital motions, and as an aid in developing other analytical expressions. Even though the hodograph presents an abstract geometry for space trajectory motion, it does augment and simplify the orbit once the investigator has become familiar with its meaning and interpretation. Quite frequently the use of a hodograph to describe a particular two-body motion provides a simplification which aids in the understanding of the problem at hand.

In this paper the hodograph of a general two-body motion will be described and several fundamental relations, as defined from this basic description, will be developed. It will be shown that the usual parameters for the hodograph can be manipulated to provide other useful results; and, that by relatively simple means the method can be employed to describe relations between the various reference angles for the flight path. In addition, it will be demonstrated that a geometrical

*Superscripts refer to references noted at the end of this paper.

development can be employed to describe the eccentric anomaly, and the mean anomaly, as these quantities relate to the position angle (or, true anomaly) for the orbit.

Basic Development

For this analysis a simple two-body, central field problem is assumed. The motion will be described in reference to two basic coordinate frames of reference – one which moves, following the motion about the trajectory; and, one which is fixed relative to the flight path proper. Let the moving frame be described by means of the moving unit triad ($\mathbf{e}_r$, $\mathbf{e}_\varphi$, $\mathbf{e}_z$), while the fixed frame will be in relation to the unit triad ($\mathbf{e}_x$, $\mathbf{e}_y$, $\mathbf{e}_z$).– See Figure 1.

In this section the basic developments will be undertaken. These will lead directly to a description of the velocity vector for the motion; and, subsequently, this expression will be utilized to describe the hodograph(s) and to obtain other useful information for relations describing the motion along the flight path.

For a description of the two-body trajectory, and that of the velocity vector, one may begin with the specific equation of motion

$$\ddot{\mathbf{r}} = -\frac{\mu}{r^2}\,\mathbf{e}_r \tag{1}$$

where μ is the gravitational constant associated with the two-body motion and $\mathbf{r}$ is the position vector, $\mathbf{r} \triangleq r\mathbf{e}_r$! If equation (1) is vectorally multiplied by $\mathbf{r}$, then

$$\mathbf{r} \times \ddot{\mathbf{r}} = -\frac{\mu}{r^2}(\mathbf{r} \times \mathbf{e}_r) \equiv 0 \tag{2}$$

since $\mathbf{r}$ and $\mathbf{e}_r$ are parallel vectors. Recognizing that

$$\mathbf{r} \times \ddot{\mathbf{r}} = \frac{d}{dt}(\mathbf{r} \times \dot{\mathbf{r}})$$

then from Equation (2)

$$\mathbf{r} \times \dot{\mathbf{r}} \triangleq \mathbf{h} \text{ (constant)} \tag{3}$$

which is the familiar expression for the (fixed) specific moment of momentum.

Next, let equation (1) be multipled (vectorally) by $\mathbf{h}$; that is,

$$\mathbf{h} \times \ddot{\mathbf{r}} = -\frac{\mu}{r^2}(\mathbf{h} \times \mathbf{e}_r) \equiv -\mu \frac{d}{dt}(\mathbf{e}_r) \tag{4}$$

wherein, it is recalled, $\mathbf{e}_r = \mathbf{r}/r$. However, since $\mathbf{h}$ and μ are constants, then an obvious first integral obtained from equation (4) would be

$$\dot{\mathbf{r}} \times \mathbf{h} = \mu(\mathbf{e}_r + \boldsymbol{\varepsilon}) \tag{5}$$

where $\boldsymbol{\varepsilon}$ plays the role of an integration constant.

When equation (5) is scalar miltuplied by $\mathbf{r}$, one obtains a form of the equation for a conic; namely,

$$r = \frac{h^2/\mu}{1 + \mathbf{e}_r \cdot \boldsymbol{\varepsilon}} \tag{6a}$$

which, when compared to the more familiar form

$$r = \frac{p}{1 + \epsilon \cos \varphi} \tag{6b}$$

leads to the conclusions that: (1) $p \triangleq$ focal parameter $= h^2/\mu$; (2) $\boldsymbol{\varepsilon}$ is the eccentricity vector, and assuming that $\varphi = 0$ corresponds to pericenter, then $\boldsymbol{\varepsilon} = \epsilon \mathbf{e}_x$. Hence $\mathbf{e}_r \cdot \boldsymbol{\varepsilon} \equiv \epsilon \cos \varphi$, which indicates that $|\boldsymbol{\varepsilon}| = \epsilon$, and $\mathbf{e}_r \cdot \mathbf{e}_x = \cos \varphi$ (See Fig. 1).

A Unique Description of the Velocity Vector

In order to describe the velocity vector for this motion, equation (5) is multiplied (vectorally) by $\mathbf{h}$; or,

$$\mathbf{h} \times (\dot{\mathbf{r}} \times \mathbf{h}) = \mu [\mathbf{h} \times (\mathbf{e}_r + \boldsymbol{\varepsilon})] . \tag{7}$$

Since, according to equation (3), $\mathbf{h} = h\mathbf{e}_z$, then it follows that the triple vector product can be replaced by

$$\mathbf{h} \times (\dot{\mathbf{r}} \times \mathbf{h}) = \dot{\mathbf{r}} (\mathbf{h} \cdot \mathbf{h}) - \mathbf{h} (\mathbf{h} \cdot \dot{\mathbf{r}}) = \dot{\mathbf{r}} (\mathbf{h} \cdot \mathbf{h})$$

since $\mathbf{h} \cdot \mathbf{r} = 0$! The vector multiplication of the right side of equation (7) can be done directly, with the resultant expression for the velocity vector being

$$\mathbf{V} = \frac{\mu}{h}(\mathbf{e}_{\varphi} + \epsilon \mathbf{e}_{y}) \tag{8}$$

which will be alternately written as $\mathbf{V} = \mathbb{C}\,\mathbf{e}_{\varphi} + \mathbf{R}\,\mathbf{e}_{y}$.

This is an expression for the velocity vector which is somewhat unusual in form—especially since the two component vectors, in the $\mathbf{e}_{\varphi}$ and $\mathbf{e}_{y}$ directions, are fixed in magnitude. It should be apparent that the full velocity vector is composed of: (1) a fixed magnitude component following the motion about the conic; and (2), a fixed vector component, relative to the orbit proper. As an aid to this description, Fig. 2 is included. Note that the vector $\mathbf{V}(\varphi) = (\mu/h)\mathbf{e}_{\varphi}$ changes direction as one moves about the orbit; however, the vector $\mathbf{V}(y) = \epsilon(\mu/h)\mathbf{e}_{y}$ is fixed in direction and magnitude for every point on the trajectory. Even though Fig. 2 is drawn as an ellipse, equation (8) is general and refers to any free, two body, central field conic.

The Velocity Components

In order to obtain the familiar speed components, in the direction of the various coordinate axes, one forms the appropriate scalar products,

using equation (8); that is, $V_i = \mathbf{V} \cdot \mathbf{e}_i (i = r, \varphi; x, y)$

or

$$V_\varphi = \mathcal{C}(\mathbf{e}_\varphi + \epsilon \mathbf{e}_y) \cdot \mathbf{e}_\varphi = \mathcal{C}\,[1 + \epsilon \cos \varphi],$$

$$V_r = \mathcal{C}(\mathbf{e}_\varphi + \epsilon \mathbf{e}_y) \cdot \mathbf{e}_r = \mathcal{C}\epsilon \sin \varphi,$$

and (9)

$$V_x = \mathcal{C}(\mathbf{e}_\varphi + \epsilon \mathbf{e}_y) \cdot \mathbf{e}_x = -\mathcal{C} \sin \varphi,$$

$$V_y = \mathcal{C}(\mathbf{e}_\varphi + \epsilon \mathbf{e}_y) \cdot \mathbf{e}_y = \mathcal{C}\,[\cos \varphi + \epsilon].$$

Note that $V_z = 0$ since $\mathbf{V} \cdot \mathbf{e}_z$ vanishes, identically.

If equation (8) is squared, then one obtains

$$V^2 \triangleq \mathbf{V} \cdot \mathbf{V} = \left(\frac{\mu}{h}\right)^2 [1 + 2\mathbf{e}_\varphi \cdot \mathbf{e}_y \epsilon + \epsilon^2] = \frac{\mu}{p} [1 + 2\epsilon \cos \varphi + \epsilon^2] \tag{10}$$

accounting for the fact that $p = h^2/\mu$. An inspection of this expression leads to the conclusion that:

for elliptic and hyperbolic motion $(1 + 2\epsilon \cos \varphi + \epsilon^2) > 0$;

and, for parabolic motion $[2\,(1 + \cos \varphi)] \geq 0$.

Recognizing that there is a limit position angle defined for motion on a hyperbolic path (i.e. as $r \to \infty$, $\varphi \to \varphi_{lim}$; $\varphi_{lim} = \cos^{-1}(-1/\epsilon)$); then the corresponding limit speed (squared) is described as,

$$V_{lim}^2 \to \frac{\mu}{p}[\epsilon^2 - 1] \equiv \frac{\mu}{a} \tag{11}$$

since $p = a(\epsilon^2 - 1)$ for the hyperbola. This last result is frequently referred to as the hyperbolic excess speed (squared). One notes that the limit speed, for a parabolic path ($\epsilon \to 1$), is

$$V_{lim}^2 \to 0.$$

Next, recalling that the eccentric anomaly ($\mathcal{E}$), for an elliptic path, can be related to the true anomaly by

$$\cos\varphi = \frac{\cos\mathcal{E} - \epsilon}{1 - \epsilon\cos\mathcal{E}} \quad \text{or} \quad \cos\mathcal{E} = \frac{\epsilon + \cos\varphi}{1 + \epsilon\cos\varphi} \tag{12}$$

then it can be shown that corresponding to equation (10), and making use of equation (7),

$$V^2 = V_c^2[1 + \epsilon\cos\mathcal{E}] \tag{13}$$

wherein $V_c^2 \triangleq \mu/r$ (local circular satellite speed (squared)). Here equations (10) and (13) relate the speed of motion on the orbit to the position angles (φ and $\mathcal{E}$). The geometric relation between φ and $\mathcal{E}$ will be described subsequently.

It should be mentioned here that the results given in equations (9) are either the usual expressions found in the literature, or are easily reduced to such results by substitution and manipulation. Also, there

is a description difference in the more familiar vector representation for velocity – note the components in equations (9) and the expression in equation (8). This last result was derived primarily for the purpose of defining the hodograph; it is not a usual equation form since it contains components which are not orthogonal (generally), and are vector elements related to both of the basic triads employed here. Figure 3 shows the various velocity elements referred to above, and some of the other geometry relative to these vector elements.

Relations Formed from the Components of Speed

Making use of the speed relations developed in equations (9) it is possible to establish several interesting analytic and geometric results – a few of these are noted in the following paragraphs. For the developments which follow here it is essential to recall, or obtain from equation (3), that

$$h = r V_{\varphi}.$$

Forming ratios of the various speed components leads to:

(1) the trajectory eccentricity,

$$\epsilon = \frac{|V_r|}{|V_x|}$$

(2) the eccentric anomaly, corresponding to a point on the trajectory, can be described as

$$\mathcal{E} = \cos^{-1}\left(\frac{V_y}{V_\varphi}\right)$$

(note equation (12));

(3) in addition to the above, it is recognized that

$$\frac{V_r V_\varphi}{V_c^2} = \epsilon \sin\varphi, \qquad \frac{V_\varphi^2}{V_c^2} = 1 + \epsilon\cos\varphi \equiv \frac{p}{r},$$

and (14)

$$\frac{V_x V_\varphi}{V_c^2} = -\sin\varphi, \qquad \frac{V_y V_\varphi}{V_c^2} = \epsilon + \cos\varphi.$$

A combination of these expressions, equation (14), yields the following:

$$1 - \frac{r}{a} = \frac{\left|\frac{V_r V_\varphi}{V_c^2}\right|}{\left|\frac{V_x V_\varphi}{V_c^2}\right|}\left(\frac{\frac{V_y V_\varphi}{V_c^2}}{\frac{V_\varphi^2}{V_c^2}}\right) \equiv \frac{|\epsilon \sin\varphi|}{|-\sin\varphi|}\left(\frac{\epsilon + \cos\varphi}{1 + \epsilon\cos\varphi}\right) \tag{15}$$

in agreement with the equation for a conic, $r = a(1 - \epsilon\cos\mathcal{E})$, when a is the semimajor axis length for the elliptic path. This last expression relates the radius (to a point on the orbit) to the speed components of a satellite. Of course, obvious reductions using these same speed components reaffirm the geometrical observation that

$$\varphi - \gamma = \frac{\pi}{2} - \beta, \tag{16}$$

where β is the elevation angle shown on Figure 3. Also, as a result of this observation, equation (15) can be alternately expressed as

$$1 - \frac{r}{a}\left[= \epsilon\left(\frac{\epsilon + \cos\varphi}{1 + \epsilon\cos\varphi}\right)\right] = \epsilon\left(\frac{\epsilon + \sin(\beta - \gamma)}{1 + \epsilon\sin(\beta - \gamma)}\right). \tag{17}$$

Equation (10) describes the local speed in terms of the position angle; to complete this description, equation (16), and a manipulation of the relation between γ and φ, namely

$$\tan\gamma \triangleq \frac{V_r}{V_\varphi} = \frac{\epsilon\sin\varphi}{1 + \epsilon\cos\varphi}, \tag{18}$$

yields the following:

$$V^2 = \frac{\mu}{p}\left[1 - 2\epsilon^2\left(\cos\beta \mp \frac{\sin\beta}{\epsilon}\sqrt{1 - \epsilon^2\cos^2\beta}\right) + \epsilon^2\right] \tag{19a}$$

and

$$V^2 = \frac{\mu}{p}\left[1 - 2\left(\sin^2\gamma \mp \cos\gamma\sqrt{\epsilon^2 - \sin^2\gamma}\right) + \epsilon^2\right] \tag{19b}$$

wherein the negative sign is used when

$$0 \leq \cos\varphi \leq -\epsilon$$

and the positive sign is employed for

$$-\epsilon \geq \cos\varphi \geq -1.$$

Note that $\cos\varphi = -\epsilon$ describes the condition $\gamma = \gamma_{max,\,min}$ for the elliptic orbit. Also, since the ellipse is speed-symmetric about the major axis, only one side of the orbit is described in the φ - relations above. For reference purposes the functional relations for $\varphi = \varphi(\gamma)$ are noted below:

$$\cos\varphi = -\frac{\sin^2\gamma}{\epsilon} \pm \cos\gamma\,\frac{\sqrt{\epsilon^2 - \sin^2\gamma}}{\epsilon}$$

and (20)

$$\sin\varphi = \frac{\tan\gamma}{\epsilon}\left(\cos^2\gamma \pm \cos\gamma\sqrt{\epsilon^2 - \sin^2\gamma}\right).$$

Equations (10), (13), and (19) express the local speed (squared) in terms of the local position angles (or anomalies) and the local elevation angles.

Other Useful Relations

Using the definition of the elevation angles (γ, β) noted with Fig. 3, it is easily shown that (see equations (9)), in addition to equation (18),

$$\tan\beta = \frac{V_y}{-V_x} = \frac{\epsilon + \cos\varphi}{\sin\varphi},$$

then it follows that

$$\tan\gamma\tan\beta = \epsilon\cos\mathcal{E}. \qquad (21a)$$

In a like manner, from the various descriptions it is evident that

$$\sqrt{1-\epsilon^2}\,\tan\gamma = \epsilon\,\frac{\sqrt{1-\epsilon^2}\,\sin\varphi}{1+\epsilon\,\cos\varphi} \equiv \epsilon\,\sin\mathcal{E}, \tag{21b}$$

relating γ, φ and $\mathcal{E}$ for any point on an elliptic trajectory.

Next, squaring and adding equations (21) leads directly to a description of the conic's eccentricity in terms of angles; namely,

$$\epsilon^2 = \frac{1+\tan^2\beta}{1+\tan^2\gamma}(\tan^2\gamma) \equiv \frac{\cos^2\gamma}{\cos^2\beta}(\tan^2\gamma)$$

and (22)

$$\epsilon = \frac{|\sec\varphi|}{|\tan\varphi - \tan\gamma|}\;|\tan\gamma|.$$

A ratio of the expressions (21) will indicate that

$$\tan\mathcal{E} = \sqrt{1-\epsilon^2}\,\cot\beta, \tag{23a}$$

while, other relations easily derived from manipulating equations (9) are:

$$\tan\varphi = \cot(\beta-\gamma)$$

or

$$\cot\beta = \tan(\varphi-\gamma) = \frac{\sin\varphi}{\epsilon+\cos\varphi} \tag{23b}$$

and

$$\tan \mathcal{E} = \sqrt{1-\epsilon^2}\, \tan(\varphi-\gamma).$$

Relating the specific energy (E) of the trajectory to the eccentricity (ϵ) it is easy to show that

$$\epsilon^2 = 1 + \frac{2E}{\mathcal{C}^2}, \text{ with } \mathcal{C} = \frac{\mu}{h}$$

then using equation (22) it is found that the specific energy is described by

$$E = \mathcal{C}^2 \frac{\tan\gamma \tan\varphi (\tan 2\gamma - \tan\varphi)}{\tan 2\gamma\, (\tan\varphi - \tan\gamma)^2}. \tag{24}$$

Also, since the specific energy for a free trajectory is known to be

$$E = -\frac{\mu}{2a}$$

then

$$a = \frac{h}{2\mathcal{C}} \left[\frac{\tan 2\gamma\, (\tan\varphi - \tan\gamma)^2}{\tan\gamma \tan\varphi\, (\tan\varphi - \tan 2\gamma)} \right]. \tag{25}$$

Finally, it should be evident that corresponding relations, expressed in terms of $\beta, \varphi\,; \varphi\,, \mathcal{E}\,; \gamma, \mathcal{E}$ are readily obtained by substitution and manipulation of the various results derived earlier.

A Description of the Hodograph

The velocity expression developed as equation (8) can be utilized, directly, for describing a hodograph corresponding to the two-body motions considered here. It will be shown that this development is amenable to either the (fixed) x, y, z – or (moving) $r, \varphi, z,$ – frames of reference noted in the introduction. Because of similarity in manipulation for the two cases it will be advantageous to conduct the developments in parallel and simultaneously:

Hodograph Referred to the r, φ, z triad. Write the velocity vector

$$\mathbf{V} = \mathcal{C}\,(\mathbf{e}_\varphi + \epsilon\,\mathbf{e}_y) \equiv V_r\,\mathbf{e}_r + V_\varphi \mathbf{e}_\varphi \,. \quad (26a)$$

Hodograph referred to the x, y, z triad

$$\mathbf{V} = \mathcal{C}\,(\mathbf{e}_\varphi + \epsilon\,\mathbf{e}_y) \equiv V_x\,\mathbf{e}_x + V_y\,\mathbf{e}_y \,. \quad (26b)$$

using equation (8); next, rearrange this result as

$$(V_\varphi - \mathcal{C})\,\mathbf{e}_\varphi + V_r\,\mathbf{e}_r = \epsilon\,\mathcal{C}\,\mathbf{e}_y. \quad (27a)$$

$$(V_y - \epsilon\,\mathcal{C})\,\mathbf{e}_y + V_x\,\mathbf{e}_x = \mathcal{C}\,\mathbf{e}_\varphi \,. \quad (27b)$$

Squaring the above expression yields

$$(V_\varphi - \mathcal{C})^2 + V_r^2 = (\epsilon\,\mathcal{C})^2 \,, \quad (28a)$$

$$(V_y - \epsilon\,\mathcal{C})^2 + V_x^2 = \mathcal{C}^2 \,, \quad (28b)$$

which describes a circle (in the V_φ, V_r plane) whose center is located at $\mathcal{C}$ units up the V_φ axis, and which has a radius of $\epsilon\,\mathcal{C}$ $(=R)$ units.

A sketch of the hodograph, and its relation to an elliptic orbit is shown as Fig. 4.

which describes a circle of radius $\mathcal{C}$; and, whose center is located at $\epsilon\,\mathcal{C}$ units up the V_y axis.

A sketch relating the hodograph to a corresponding ellipse is noted in Fig. 4.

The geometries of Fig. 4 have been chosen to represent the elliptic orbital motion, with convenience of representation being the factor deciding for this case. It should be evident, however, that the descriptions could have been made for the hyperbolic case just as well. As a

matter of fact, to illustrate this companion situation, and to indicate the relative geometries corresponding to the hyperbolic trajectory and to the special cases of the circle and the parabola, the following figure (Fig. 5) has been prepared.

The cases illustrated in Fig. 5 show a comparison of the hodograph, for several values of eccentricity, as they would appear on the two velocity planes (V_r, V_φ ; V_x , V_y). It should be noted that the circular orbit, in the V_r , V_φ plane, is the point, $\mathcal{C}$; while in the V_x , V_y plane the hodograph is a circle of radius $\mathcal{C}$ with its origin at the origin of coordinates (i.e. $\epsilon = 0$, hence $R = 0$). As the eccentricity increases the figure of the hodograph grows, in size, in the V_r , V_φ plane; while for the V_x , V_y plane the origin of the figure moves away from the coordinate origin. When the trajectory is a parabola the two geometrics appear to be the same ($\mathcal{C} \equiv R$; $\epsilon = 1$). For the hyperbola, since $\epsilon > 1.0$, the hodograph (circle) in the V_r , V_φ plane has a radius (R) which is greater than the center's location position ($\mathcal{C}$), hence the figure extends into the negative V_φ region, which is, of course, unrealistic. This same case, referred to the V_x , V_y plane, is represented by a circle whose center lies well above the origin; and, whose unrealistic portion (of the hodograph) appears as the cross-hatched region shown in Fig. 5. (The angle φ_{lim} is described by $\varphi_{lim} = + \cos^{-1} (- 1/\epsilon)$!).

It should be evident that for comparable cases (using consistent and fixed values for $\epsilon, \mathcal{C}$) the V_x , V_y hodograph is most useful, from a geometrical-size consideration, for small eccentricities (near zero);

note that the radius of the hodograph is fixed so long as $\mathcal{C}$ is fixed. However, in the V_φ, V_r plane the center's position is constant for a given fixed value of $\mathcal{C}$.

Geometric Description of the Eccentric Anomaly, $\mathcal{E}$

Figure 6, shows, in schematic, the eccentric anomaly ($\mathcal{E}$) and the corresponding true anomaly (φ) for a representative position, P, on an elliptic trajectory. The point, P', lies on the so-called auxiliary circle (of radius, a) and corresponds to the trajectory point, P; position coordinates for these two points are $(a, \mathcal{E})$ and (r, φ), respectively. In this section a geometric method for determining $\mathcal{E}$, from the hodograph, will be described; in fact the construction for both the hodograph planes mentioned before will be described.

Hodograph on the V_r, V_φ Plane

For the hodograph referred to the V_r, V_φ plane the speed components (equation (9)) are

$$V_r = \epsilon \mathcal{C} \sin \varphi$$

and

$$V_\varphi = \mathcal{C} (1 + \epsilon \cos \varphi). \tag{29}$$

Let a modified hodograph be described, one whose coordinates are $V_r/\mathcal{C}$ and $V_\varphi/\mathcal{C}$. This modification leaves the basic geometry unchanged even though the relative scale of the figure is altered. For this representation the hodograph is a circle whose radius is equal to the trajectory's eccentricity, and with its center at a unit distance from the coordinate origin.

Recalling that the eccentric anomaly may be expresed by

$$\cos \mathcal{E} = \frac{\epsilon + \cos \varphi}{1 + \epsilon \cos \varphi} \tag{30}$$

then the following construction, based on this relation, determines this position angle. The various steps in the construction are seen on Fig. 7 and are listed below:

1. Draw a (modified) hodograph on the $V_r/\mathcal{C}$, $V_\varphi/\mathcal{C}$ plane; this is a circle of radius equal to the eccentricity, and has its center at a unit distance up the $V_\varphi/\mathcal{C}$ axis (see equation (28a)). The center of the hogograph is at 0.

2. P is the point of interest on the trajectory; it is located by φ (position angle, or true anomaly), and/or by $\mathcal{E}$, the eccentric anomaly (recall Fig. 6).

3. Using 0 as a center, draw a unit circle and extend 0P to locate Q (on the unit circle). Note the $0P = \epsilon$ (units) while $0Q = 1$ (unit).

4. Project P onto the $V_r/\mathcal{C}$ axis – this locates point D; thus, the distance $PD = 00' + 0P \cos \varphi$, or, $PD = 1 + \epsilon \cos \varphi$.

5. Project Q onto the $V_\varphi/\mathcal{C}$ axis, locating Q_1; then $0'Q_1 = 1 + \cos \varphi$.

6. Extend the line QP0; then, using 0 as a center, transfer point Q_1 to QP0 (extended) locating point Q_2.

Since $0Q = \cos \varphi$, the $\underline{\underline{PQ_2}} = 0P + 0Q_2 = \underline{\underline{\epsilon + \cos \varphi}}$.

7. At Q_2 erect a perpendicular (to $P0Q_2$); and, using P as a center transfer D to D_1 (where the arc of radius PD cuts the perpendicular from Q_2).

Since $PD = 1 + \epsilon \cos \varphi$, then $\underline{\underline{PD_1 = 1 + \epsilon \cos \varphi}}$.

8. According to equation (30) the angle at P, between PQ_2 and PD_1, is the eccentric anomaly - corresponding to the point P on the trajectory.

This, essentially, completes the construction. However, before leaving this discussion note that the line through 0, perpendicular to PD_1, and locating J, describes a line whose length is

$$0J = \epsilon \sin \mathcal{E}, \tag{31}$$

recognizing that $0P = \epsilon$. The significance of this will be noted subsequently.

Also, for convenience, it is helpful to relocate the eccentric anomaly (relative to 0); this is easily accomplished by erecting perpendiculars, though 0, to the lines PQ_2 and PD_1. This last construction is illustrated on Fig. 8.

It should be evident that the arc P_1Q corresponds to the position angle (φ) while the arc AA_1 refers to the eccentric anomaly ($\mathcal{E}$); both arcs are comparable since they are segments of the unit circle.

Hodograph on the V_x , V_y Plane

For the hodograph described on the V_x, V_y plane the speed components are known to be,

$$V_x = -\mathcal{C} \sin \varphi,$$

and (32)

$$V_y = \mathcal{C} (\epsilon + \cos \varphi),$$

(see equations (9)).

As in the previous case it is advisable to work on a modified hodograph plane. Here the coordinate axes will be chosen as $V_x/\mathcal{C}$ and $V_y/\mathcal{C}$, respectively. This will simplify the construction for $\mathcal{E}$, while retaining the basic geometry of the hodograph proper. Once again the construction will be based on equation (30); while the steps to be followed are noted below and pictured on Fig. 9.

The construction on this plane is much simpler than that for the previous case. Here the hodograph is represented by a circle of unity radius; P is the reference point on the (elliptic) orbit, defined by the position angle φ.

1. Project P onto the $V_y/\mathcal{C}$ axis locating P_1.

Since $0P = 1.0$, then $0P_1 = \cos \varphi$. Also, note that $\underline{\underline{0' P_1}} = 0'0 + 0P_1 = \underline{\underline{\epsilon + \cos \varphi}}$, since $0'0 \equiv \epsilon$.

2. Erect a perpendicular, to the line 0P (extended), through 0'; this will locate the point Q.

Since $00' = \epsilon$, then $0Q = \epsilon \cos \varphi$ and $\underline{\underline{PQ}} = P0 + 0Q = \underline{\underline{1 + \epsilon \cos \varphi}}$.

3. Using $0'$ as a center, and PQ as a radius, swing an arc locating point **D** as the intersection of this arc (radius PQ) with the line PP_1.

Now, the eccentric anomaly ($\mathcal{E}$) is noted to be the angle at $0'$ in the triangle whose base is $0'P_1$ and whose hypotenuse is $0'D$, as shown.

4. Note that the perpendicular erected through 0, drawn normal to $0'D$ (locating point J) describes a line whose length is

$$0J = \epsilon \sin \mathcal{E}.$$

The significance of $0J$ will be discussed subsequently.

For the convenience of comparison, the angle $\mathcal{E}$ is transferred to the origin (0) so that it is directly related to the corresponding true anomaly (φ) – thus, in Fig. 9b, the arc $\mathcal{P}A$ relates to $\mathcal{E}$, while the arc $\mathcal{P}P$ relates to φ; both angles correspond to the position point, P, on the ellipse. Also, for convenience, the length $0J$ has been transferred to the horizontal as noted on Fig. 9b.

The Time Equation

It can be shown readily, and is well known, that the time of flight from pericenter along an elliptic path, expressed in terms of the eccentric anomaly, is

$$n(t - \tau) = \mathcal{E} - \epsilon \sin \mathcal{E}, \tag{33}$$

where n is the mean motion and τ is the time of pericenter passage. Referring back to the construction for the eccentric anomaly, it should be apparent that all of the information needed to describe the time of flight has been determined within those geometric manipulations. The arc relating to $\mathcal{E}$, and the line 0J (= $\epsilon \sin \mathcal{E}$) have been constructed; thus by subtracting these two numbers – one describing the arc for $\mathcal{E}$, the other being the length 0J – the time function $n(t - \tau)$ is determined.

As an alternate description, the length 0J can be converted to an equivalent angle (since the basic hodograph geometry has been referred to a unity circle) so that the difference between $\mathcal{E}$ and this equivalent angle represents $n(t - \tau)$. It is usual to refer to this angle difference as the Mean Anomaly (M).

In connection with these statements a modified hodograph diagram, showing the relative sizes of the angles ($M, \mathcal{E}, \varphi$), is presented as Fig. 10. On the figure are several (corresponding) angular combinations; these are shown to indicate the relative extent of the various angles and their corresponding relative variations as one progresses about the elliptic orbit. These sets of angles are denoted as φ_i, $\mathcal{E}_i$, M_i (i being the indicator index) on the figure.

CONCLUSIONS

The developments carried out in the foregoing paper have illustrated the utility of the hodograph as a means of deriving useful analytical expressions, and as a valuable geometric tool for describing

various aspects of two-body motions. If the usual hodographic representation is altered, and a modified form of the hodograph is described, it is found that a graphical means for determining the eccentric anomaly is obtained. In addition, from this same construction one is able to obtain the information, geometrically, to describe the time of flight (from pericenter) to a point of interest on the trajectory of motion.

These few examples illustrate some of the uses of the hodograph, not just as a geometric check on analytic results, but also as a means for the development, and frequently the simplification, of analytic relations. Once this technique is mastered it should prove to be a most helpful adjunct to the more usual tools employed in trajectory design and analysis.

REFERENCES

1. Altman, S. P. Orbital Hodograph Analysis, Vol. 3, AAS Science and Technology Series, Western Periodicals, 1965.

2. Altman, S. P. and Pistiner, J. S., "Hodograph Analysis of the Orbital Transfer Problem for Coplanar Nonaligned Elliptical Orbits", ARS Journal Vol. 31, September 1961.

3. Sun, F. T., "On the Hodograph Method for Solution of Orbital Probblems", Proceedings of the 12th International Astronautical Congress, Academic Press, New York, 1963.

4. Eades, J. B. The Hodograph and Its Application to Space Flight, Bulletin No. 157, Virginia Engineering Experiment Station, VPI, Blacksburg, Virginia, December 1964.

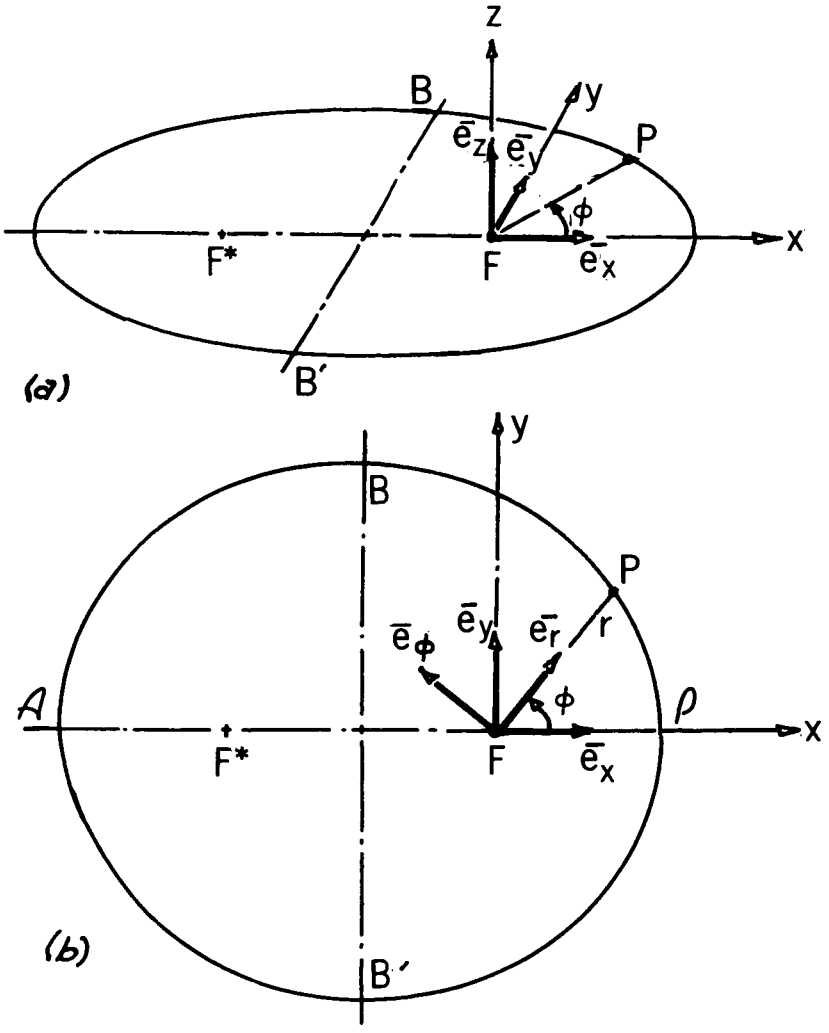

Figure 1 – The basic geometry for a two-body (elliptic) trajectory, showing two representative frames of reference (x, y, z-fixed frame; and, r, φ, z-moving frame). The description in sketch (a) is a three-dimensional representation showing the unit triads, with the $\mathbf{e}_z$ vector being normal to the orbital plane. Sketch (b) describes the plane of motion showing the basic relations between the in-plane coordinates, (x, y) and (r, φ). Point P is a general point on the ellipse; F and F* are the occupied and unoccupied foci, respectively; the line BB′ is the minor axis for the figure.

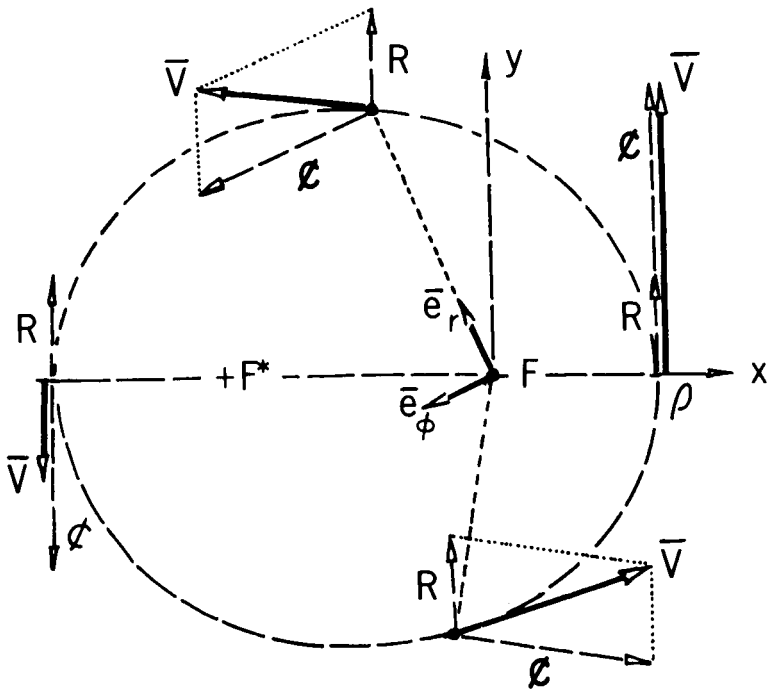

Figure 2–A sketch showing the composition of the velocity vector, for a central field conic as

$$\mathbf{V} = \frac{\mu}{h}(\mathbf{e}_\varphi + \epsilon\,\mathbf{e}_y) = \mathbf{V}(\varphi) + \mathbf{V}(y)$$

wherein $$\mathbf{V}(\varphi) = \frac{\mu}{h}\,\mathbf{e}_\varphi \equiv \mathbb{C}\,\mathbf{e}_\varphi$$

and $$\mathbf{V}(y) = \epsilon\,\frac{\mu}{h}\,\mathbf{e}_y \equiv \mathbf{R}\,\mathbf{e}_y$$

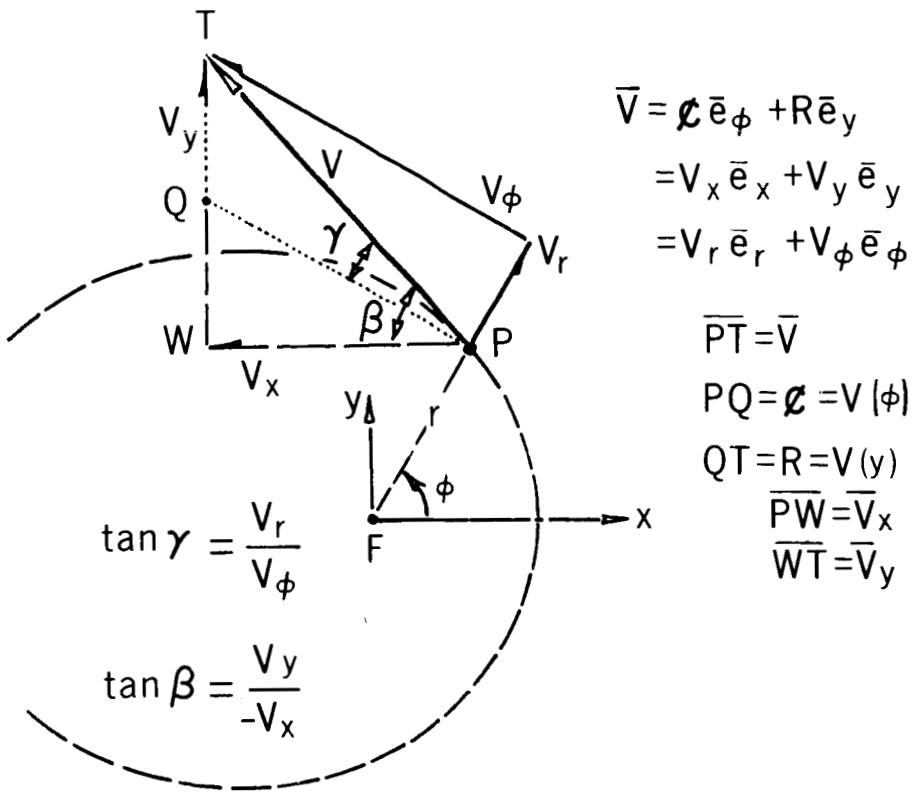

Figure 3–Velocity Components and Velocity Elements. Also shown here are the elevation angles (γ, β) used to locate the velocity vector relative to the two triad of interest; namely ($\mathbf{e}_i$, $\mathbf{e}_\varphi$, $\mathbf{e}_z$) and ($\mathbf{e}_x$, $\mathbf{e}_y$, $\mathbf{e}_z$).

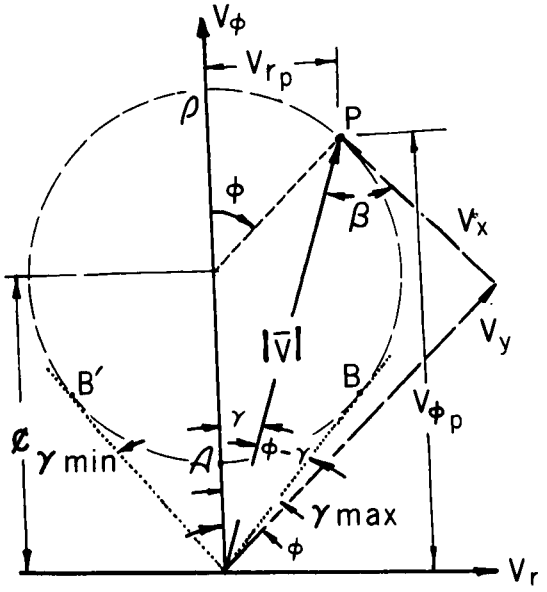

(a) Hodograph on the V_r, V_φ plane

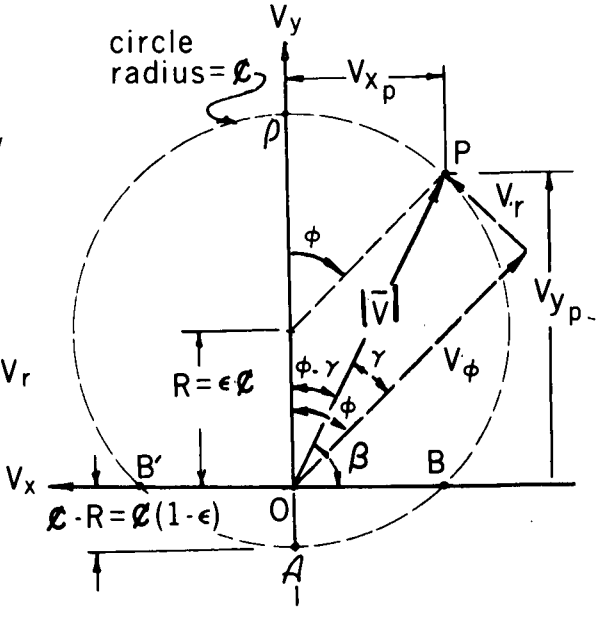

(b) Hodograph on the V_x, V_y plane

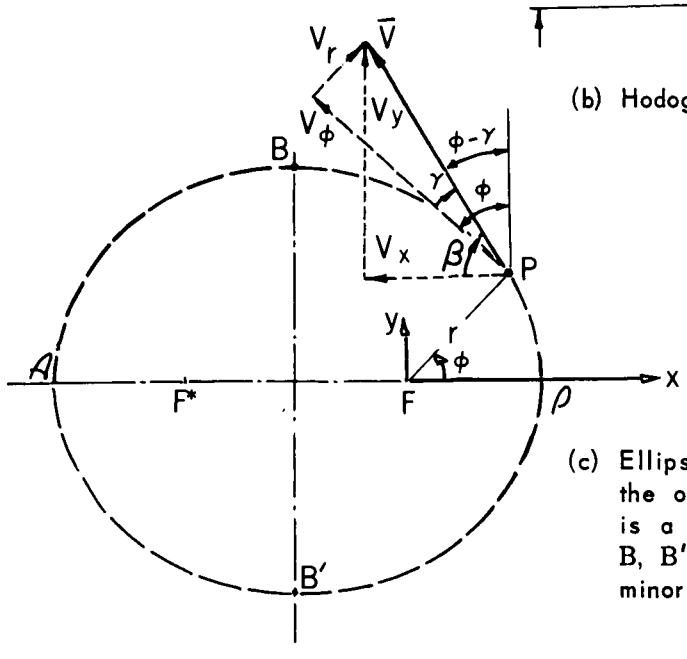

(c) Ellipse of motion (F, F^* represent the occupied, unoccupied foci; P is a general point in the ellipse; B, B′ represent the extent of the minor axis).

Figure 4 – Sketch of the hodograph(s), corresponding to an ellipse of motion, on the V_r, V_φ, plane and on the V_x, V_y plane. The positions noted as ℙ, 𝔸, represent pericenter and apocenter, respectively. Shown on both hodographs are the velocity components and reference angles corresponding to each figure, providing a correlation of these representations.

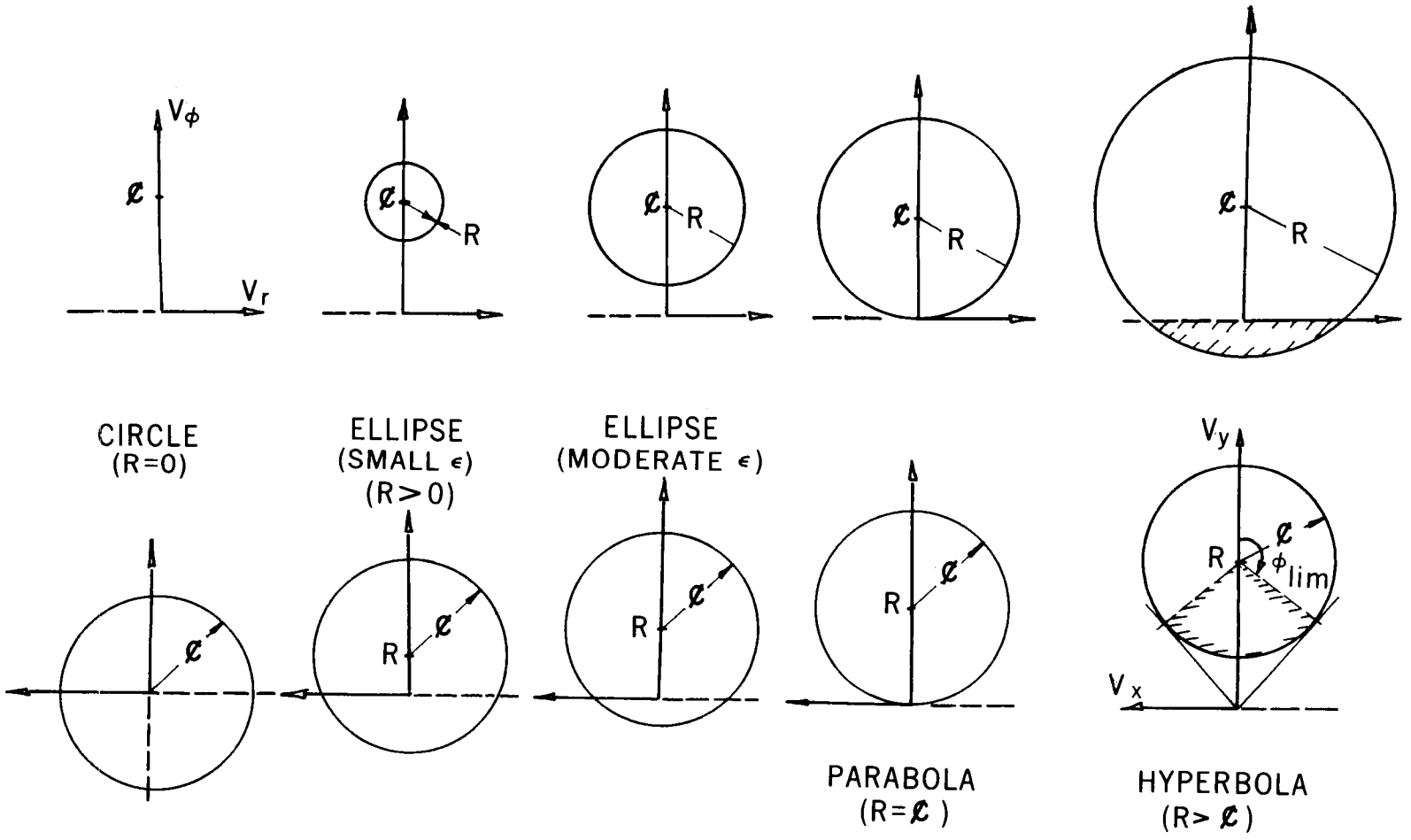

Figure 5 – Sketch showing the relative geometries of the hodographs, for a given motion, on the V_r, V_φ and V_x, V_y planes. For purposes of comparison a constant value of $\mathcal{C}$ has been assumed here. Note that the trajectories have been varied from circles to hyperbolas.

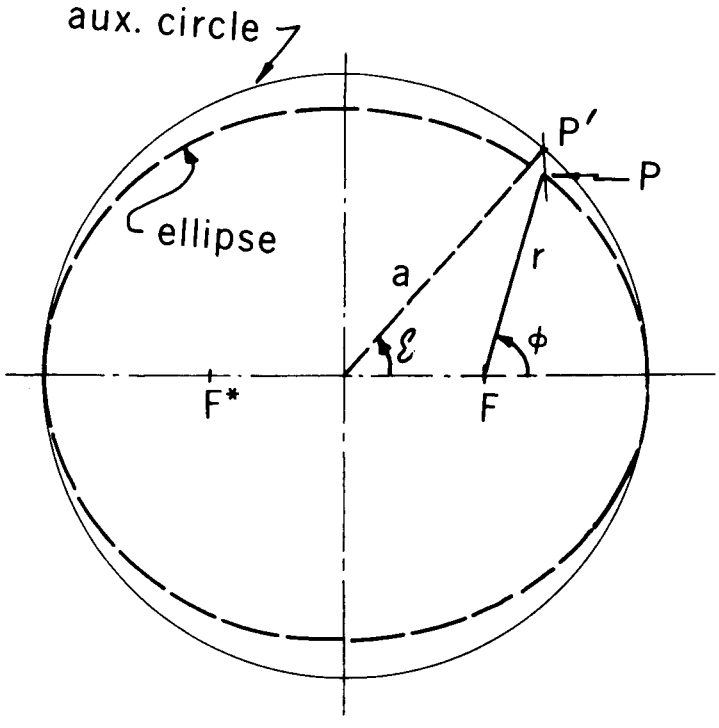

Figure 6–Sketch showing an elliptic trajectory and the corresponding auxiliary circle.

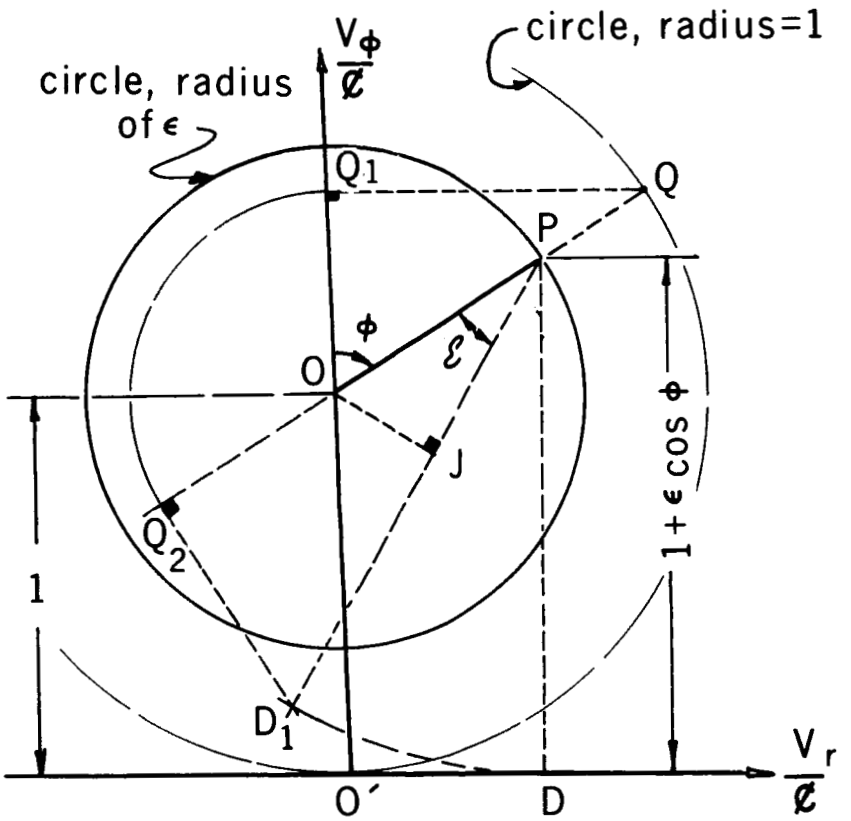

Figure 7–The modified hodograph and a graphical description of eccentric anomaly, $\mathcal{E}$.

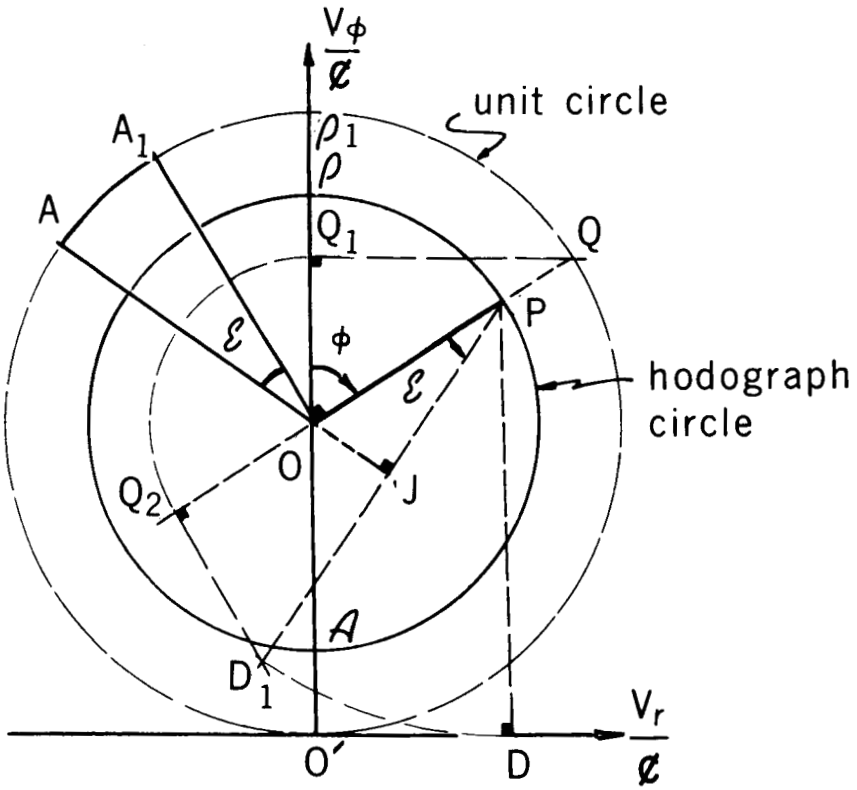

Figure 8 – Relocation of the eccentric anomaly, relative to the hodograph origin, 0. The arc AA_1 indicates $\mathcal{E}$ (P), while the arc from $\mathcal{P}$ to Q represents φ (P).

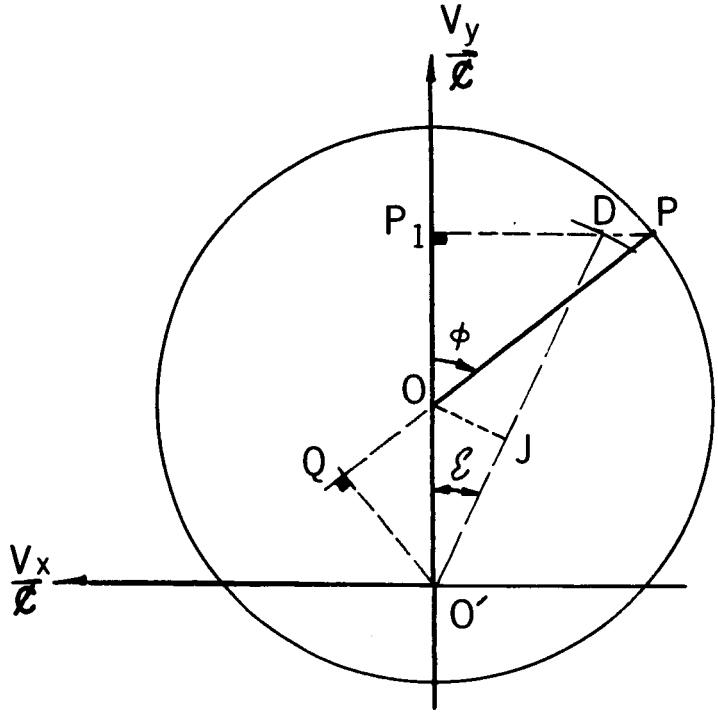

Figure 9(a)—The V_x, V_y hodograph construction for the eccentric anomaly.

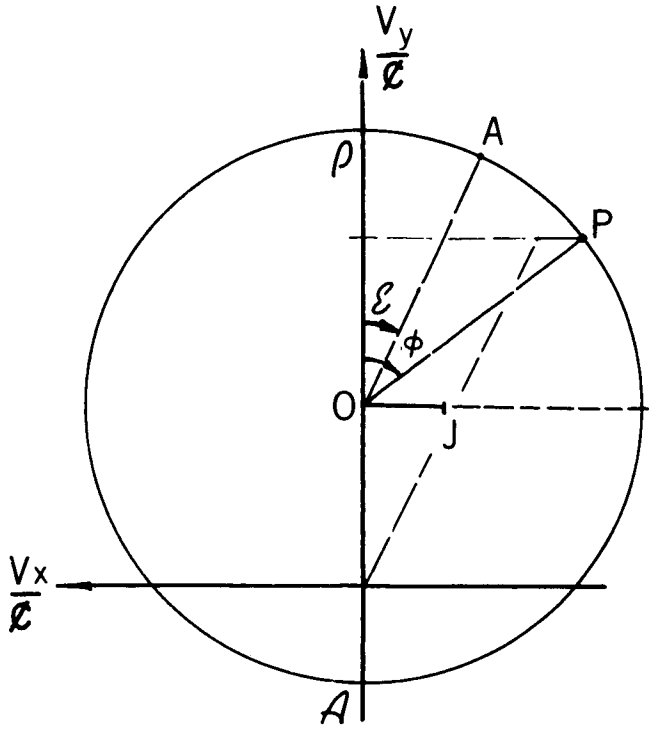

Figure 9(b)—The relocation of $\mathcal{E}(P)$ relative to the hodograph origin, O.

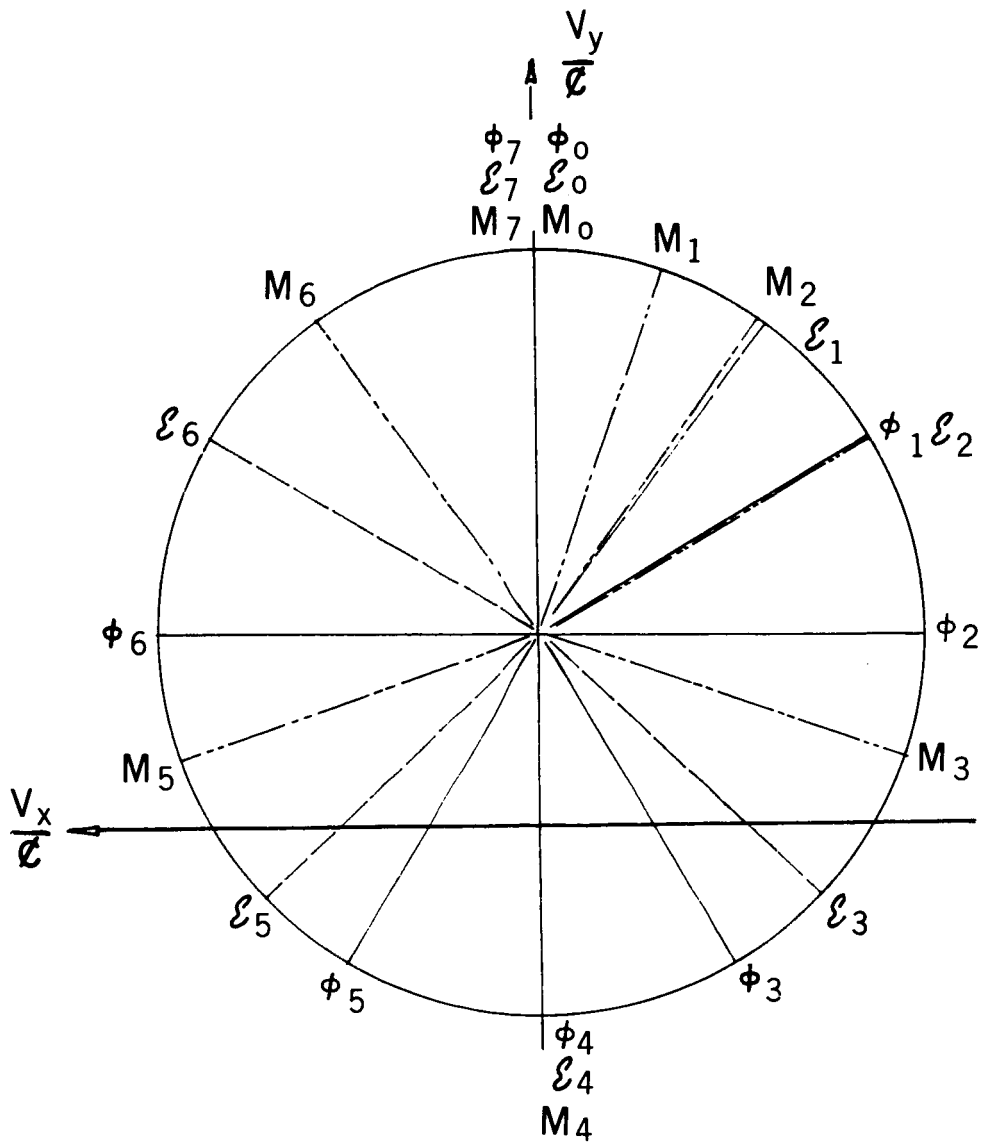

Figure 10 – A graphical representation of the angles φ, $\mathcal{E}$, M on a modified hodograph in the $V_x/\mathcal{C}$, $V_y/\mathcal{C}$ plane. The indices on each angle set are used to correlate the various angle sets.